# DEVELOPMENT OF A NOVEL INTELLIGENT SPEED ADAPTATION SYSTEM BASED ON AVAILABLE SIGHT DISTANCE

*Original*
DEVELOPMENT OF A NOVEL INTELLIGENT SPEED ADAPTATION SYSTEM BASED ON AVAILABLE SIGHT DISTANCE / Hazoor, A.; Lioi, A.; Bassani, M.. - In: TRANSPORTATION RESEARCH RECORD. - ISSN 0361-1981. - ELETTRONICO. - 2675:9(2021), pp. 1573-1584. [10.1177/03611981211008885]

*Availability:*
This version is available at: 11583/2906236 since: 2021-06-11T14:23:35Z

*Publisher:*
Transportation Research Board of the National Academies

*Published*
DOI:10.1177/03611981211008885

# DEVELOPMENT OF A NOVEL INTELLIGENT SPEED ADAPTATION SYSTEM BASED ON AVAILABLE SIGHT DISTANCE

**Abrar HAZOOR**
Department of Environment, Land and Infrastructure Engineering
Politecnico di Torino, Torino, Italy, 10129
Email: abrar.hazoor@polito.it
ORCID: 0000-0002-4963-056X

**Alessandra LIOI**
Department of Environment, Land and Infrastructure Engineering
Politecnico di Torino, Torino, Italy, 10129
Email: alessandra.lioi@studenti.polito.it
ORCID: 0000-0003-0812-4094

**Marco BASSANI**
Department of Environment, Land and Infrastructure Engineering
Politecnico di Torino, Torino, Italy, 10129
Email: marco.bassani@ polito.it
ORCID: 0000-0003-2560-1497

Word Count: 4,875 words + 2 table (250 words per table, 500) = 5,375 words

*Submitted [July 24th, 2020]*

*Re-submitted [November 23rd, 2020]*

## ABSTRACT

Roads are designed without considering the improved performance of modern vehicles and the new onboard technologies available for assisted driving. In addition, vehicles frequently travel at speeds which exceed the maximum considered in road design. Hence, the need for speed and safety related countermeasures (e.g., field control, mobile or fixed speed cameras, traffic calming measures) is evident. However, such countermeasures are proving ineffective, and the proportion of crashes which are speed-related remains significant.

This investigation is aimed at the development of a new Intelligent Speed Adaptation (ISA) system based on the available sight distance (ASD). In conditions of poor sight distance available, the system may (i) inform drivers when they are travelling at inappropriate speeds in conditions of poor visibility, or (ii) generate warning sounds to the same effect, or (iii) intervene directly and compel drivers to adopt the speed which is most appropriate to the particular ASD. In this methodological paper, the functionality of the new ISA system has been tested at the driving simulator of the Politecnico di Torino (Italy). The estimation in the virtual environment of the ASD has been validated and tested successfully. Future experimental investigations will be devoted to assessing the effectiveness of the system on driver speed behavior and decision making.


**Keywords:** speed management, intelligent speed adaptation, driver behavior, available sight distance, stopping distance.

## INTRODUCTION

Although vehicles and roads form part of the same transportation system, their design and development follow different disciplines, with the result that opportunities for greater cooperation at the design stage of the two components are rare (*1*,*2*). One of the biggest issues in the highway system is that of speed management. Speed is the factor that more than any other influences design (i.e., the design speed), traffic operations (i.e., the operating speed), and safety (i.e., speed at collision).

In traffic safety literature, the relationship between speed and crash frequency/severity is established and can be broken down into pre-event and event phases (*3*). In the first, the increase of speed corresponds to a higher probability of crash occurrence (i.e., the higher the speed, the longer the distance required to stop the vehicle and the lower the probability of avoiding collisions). Data and models reported in scientific literature support this evidence (*4*,*5*). In the second, damages to vehicle and injuries to the road users involved are proportional to the kinetic energy (E) released in the collision, and consequently to the squared value of the pre-crash speed.

To discourage excessive speeds, police and automated enforcement (e.g., speed cameras) and engineering solutions (e.g. road signs and markings, rumble strips, speed humps, road narrowing, etc.) may be adopted (*6*). However, these measures are only partially effective (*7*-*9*), with any positive effects limited to those road sections and immediate surroundings where the measures were adopted (*10*). Literature confirms that such systems prove ineffective in locations distant from the treated ones due to migration phenomena (6,*11*-*13*).

In contrast, onboard vehicle technologies may be more effective and provide better results since they remain continuously in operation on the vehicle. Carsten and Tate (*14*) predicted several positive effects with Intelligent Speed Adaption (ISA) systems on new vehicles, ranging from a reduction in both crash frequency and severity, and a decrease in fuel consumption. ISA can act in a number of ways: it can (i) inform, (ii) warn the driver, or (iii) intervene directly on pedals and temporarily prevent the driver from making any speed decisions (*15*). Since intervening ISA systems can be deactivated (*7*), different speed behaviors emerge between drivers who leave the system operational and those who deactivate it. Evidence from Lai and Carsten (*16*) indicates that those who prefer to deactivate it get the best benefits if they use it.

## PROBLEM STATEMENT

Current ISA technologies use speed databases or recognize vertical signs bearing speed limit information for a roadway segment (*9*). The posted speed limit on a road segment is based on general values from national highway rules and, more specifically, on the road category and is designed to guarantee mobility and safety for all road users and an overall acceptable level of environmental protection (*17*). The established reference limits can then be modified at a local level in response to factors that increase the crash risk, i.e. wet/icy road pavement conditions, limited visibility, conflicts with other road users, hazardous conditions along the roadside (*18*,*19*). However, differences between operating and posted speeds may be due to limited credibility of traffic signals (*20*,*21*). Some road factors may reduce the driver's risk perception and promote higher speeds (e.g., wider lanes, a high number of lanes, high visibility conditions) with the result that a consistent number of drivers exceed the speed limit.

In many other cases, the presence of permanent or temporary sight obstructions limits the sight distances available to the driver, with the result that he/she has to decide on the best speed to adopt to maintain the distance necessary for a sudden emergency stop (i.e., the stopping distance, *SD*) lower than the visible distance along the future trajectory (i.e., the available sight distance, *ASD*). When $SD < ASD$, the driver operates under safe visibility conditions. Accordingly, when negotiating a curve with limited visibility, drivers may perceive a risk due to unknown conditions along that part of the curve that they cannot see.

However, the sight distance assessment is not accounted for by some road agencies in the evaluation of a safe speed limit, with the result that even drivers who are respecting the posted limit can drive unsafely (*22*). Furthermore, in several temporary or new road scenarios, permanent sight obstructions may further reduce the *ASD* with respect to the designed value (*23*,*24*). In road scenarios with limited *ASD*, drivers have the opportunity to reduce their speed to safer levels. Bassani et al. (*25*) observed that some drivers use compensatory strategies in response to the perceived risk of sight limitations to let *SD* < *ASD*: they reduce their speed to restrict the *SD*, or move laterally to benefit from an increased *ASD*. However, a significant percentage of drivers do not perform any compensatory maneuver and, thus, they negotiate the curves at an excessive speed and travel under partially or totally unsafe sight conditions (*SD* > *ASD*). One explanation for excessive speeds at road curves can be a false perception of the roadway ahead. **Table 1** exhibits the percentage of curve negotiations under safe, partially, and totally unsafe conditions and the range of compensatory strategies exhibited by a group of test drivers in the driving simulation study from Bassani et al. (25). The terms are defined as follows:

(i) safe conditions, when drivers travel under good visibility (i.e., above sight distance criteria) along a curve with *ASD* always > *SD*;

(ii) partially safe conditions, when drivers enter and exit a curve with ASD > SD but encounter poorer visibility conditions (ASD < SD) at the middle section of that curve (i.e., below sight distance criteria), albeit the visibility conditions might be sufficient for safe transit when one considers that sight distance equation assumptions have a generous margin of safety; and

(iii) unsafe conditions, when drivers negotiate a curve with ASD < SD along the full length of the curve (25).

**TABLE 1 Driver choice of compensatory strategy combinations considering visibility conditions along curves with limited sight distance available (*25*).**

| **Visibility condition** | **Strategy** | | | |
|---|---|---|---|---|
| | **Lateral Shift** | **Speed Reduction** | **Both** | **None** |
| **Safe (*ASD* > *SD*)** | 11.5% | 36.9% | 3.5% | 48.1% |
| **Partially Safe** | 18.9% | 40.3% | 6.6% | 34.1% |
| **Unsafe (*ASD* < *SD*)** | 5.8% | 49.3% | 26.1% | 18.8% |
| **Total** | 14.0% | 38.8% | 5.9% | 41.3% |

## RESEARCH OBJECTIVE

This work presents the development of a new ISA system based on road geometrics and sight conditions. The new ISA functionality is based on an algorithm developed by referring to the following condition for road design (*26*,*27*):

$$SD(v, f, i) \leq ASD(s) \quad (1)$$

where *SD* is the stopping distance which depends on vehicle speed (*v*), the available friction between tires and pavement (*f*), and the longitudinal grade (*i*). In **Equation 1**, *ASD* is the real-time available sight distance at a specific station (*s*). **Equation 1** is used by road designers to assess safety conditions in the geometric design of highways (*26*,*27*).

In this study, the new ISA is proposed in three variants following the classification compiled for the Advanced Driver Assistance System (ADAS) (*15*,*28*,*29*): (i) informative and (ii) warning ISA operations, which enable drivers to maintain a safe speed via the activation of visual or acoustic signals respectively whenever the vehicle exceeds the speed limit; and (iii) an intervening ISA operation in which the vehicle speed is controlled by ensuring that the maximum possible pressure that may be exerted on the throttle pedal is calibrated to prevent the vehicle from exceeding the threshold speed limit, with this speed limit displayed to the drivers.

The main aim of this manuscript is to present the initial activities related to (i) the implementation of the sensors able to detect the *ASD* in the virtual environment and its validation, (ii) the development of the algorithm for three ISA variants, (iii) the implementation of the MATLAB Simulink® co-simulation framework for the application of the ISA variants at the driving simulator, and (iv) the test of the ISA variants at the driving simulator.

Applications for real vehicles of this new ISA technology are possible due to the simultaneous research works already carried out on the dynamic evaluation of the available sight distance. For example, Jung et al. (*24*) evaluated the farthest point visible from the driver's point of view with lidar point cloud data. They reconstructed the 3D space visible as the space reachable with a linear line of sight from a moving observer. Further updates of the system that they developed will facilitate the transfer of the system here from a virtual to the real road environment.

# METHODS

## Apparatus

This study was conducted with a fixed base driving simulator equipped with a force-feedback steering wheel, pedals, dashboard, adjustable seat, and manual gearbox. Three 32-inch screens with a resolution of 1920×1080 pixels having a frequency of 60 Hz were employed to project the simulated environment onto a 130° horizontal field of view. A speedometer was also inserted into a dashboard placed behind the steering wheel. Moreover, a 5.1 surrounding sound system provided realistic car engine, road, wind, and other environmental background noises. SCANeR Studio® software was used for the development of simulated road scenarios and to run the simulation. Previous studies involving this simulator found relative validation for the driver speed decision (*30*,*31*), for trajectories (*32*), and driving operations (*33*).

The software provides the module and tools for the sensor simulation within the virtual environment. In this study, a "virtual sensor" was mounted in the vehicle having a 120°×60° field of view (viewing angle) in the horizontal and vertical directions respectively. This virtual sensor provides complete information on the visibility of the road surface in the virtual environment with respect to the road markers placed along the lane centerline. The distance between the farthest marker visible from the virtual sensor and the vehicle provides the *ASD* (**Figure 1a**).

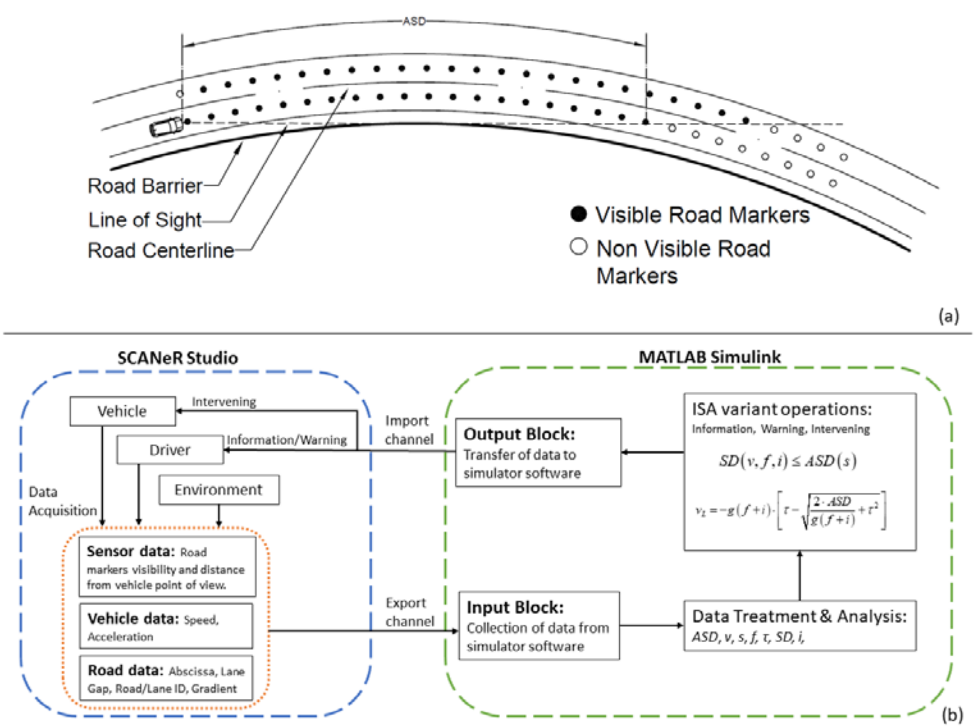


**Figure 1 Road Sensor points on the alignment visible from the vehicle (a), and interaction between SCANeR Studio® and MATLAB Simulink® co-simulation framework (b).**

There are two factors to consider regarding the positions of the road markers: (i) number, and (ii) distance between consecutive markers. The distances between the vehicle and the markers were extracted and further analyzed in the MATLAB Simulink® model to estimate the *ASD*.

**Algorithm**

For the application of **Equation 1**, the driver simulator software was co-simulated with MATLAB Simulink® in a 'Driver In the Loop' (DIL) model (*34*). The vehicle dynamic, road environment, and sensor data are transferred in real-time from SCANeR Studio® to Simulink® as per the co-simulation workflow framework between the two pieces of software (**Figure 1b**).

The data execution frequency of MATLAB Simulink® model was set at 100 Hz, while a lower frequency (20 Hz) was set for the output message sending frequency to avoid network overload. As mentioned previously, the three ISA variants were developed in MATLAB Simulink®.

*Information (ISA variant-1) and Warning (ISA variant-2) operation*

The first two ISA variants operate by comparing the *ASD* and *SD* values as elaborated previously in **Equation 1**. Since the *ASD* is estimated by processing the sensor data in real-time using MATLAB Simulink®, a data treatment block was included in the Simulink model to locate the farthest visible point along the driving lane centerline.

The exact real-time value of *SD* in the case of an emergency stop was estimated by assigning the following equation in the Simulink model:

$$SD = v \cdot \tau + \frac{v^2}{2g \cdot (f \pm i)} \tag{2}$$

The equation measures the most probable distance required to stop the vehicle considering two components: the lag distance, used to perceive and react to commands, and the braking distance to a complete vehicle stop. In **Equation 2**, $v$ is the real-time vehicle speed in m/s, $\tau$ is the perception and reaction time in s (estimated with 2.8 - 0.01 · $V$, with $V$ the speed in km/h), $f$ is the tire-road friction coefficient, $g$ is the gravitational acceleration, and $i$ is the longitudinal grade of the road (*27*). Regarding the tire-road friction coefficient, safe values for wet pavement conditions provided by the Italian standard as a function of vehicle speed were used. It is worth noting that the Italian policy considers that when a significant amount of lateral friction is used for vehicle stability (e.g., along tight curves), the available longitudinal friction is reduced. In particular, the standard assumes a reduction in longitudinal friction consistent with the friction ellipse concept. Finally, the friction values used in **Equation 2** were based on real-time vehicle speed through the Simulink model.

In the case of Informative ISA variant-1, an icon recommending a reduction in speed was displayed in front of the driver (i.e., on the windscreen). With the auditory Warning ISA variant-2, a sound was emitted to indicate that the ASD value had fallen below the estimated *SD* (**Equation 2**).

*Intervening (ISA variant-3) operation*

The Intervening ISA (variant-3) operation prevented the vehicle exceeding a threshold speed limit ($v_L$) that satisfies **Equation 1**. For this reason, the threshold speed limit along the road in real-time was calculated by replacing the *SD* with the *ASD* in **Equation 2**, and the speed limit ($v_L$) was defined as follows:

$$v_L = -g(f+i) \cdot \left[ \tau - \sqrt{\frac{2 \cdot ASD}{g(f+i)} + \tau^2} \right] \tag{3}$$

where the friction coefficient ($f$) and perception reaction time ($\tau$) were calculated using real-time vehicle speeds. The intervening model operates in two additional ways: (i) it activates if the vehicle speed is higher than the estimated threshold speed at which point it automatically decreases the speed steadily and gradually back to the threshold limit, and (ii) if the driver accelerates the vehicle from a safe condition to an unsafe condition it maintain the vehicle speed at the $v_L$ value.

## ISA VALIDATION

A two-lane road alignment with a lane width of 3.5 m and a shoulder width of 0.5 m was designed to test the model. The horizontal alignment was made up of eleven curves and designed in such a way that each curve was followed by a smaller radius as listed in **Table 2**. The vertical alignment was assumed to be flat (i.e., null gradient). The horizontal arcs were placed between two transitional spiral curves designed according to the Italian Geometric Design Standards (*27*). To limit the *ASD* values along curves, a sight obstruction in the form of a series of 950 mm high safety barriers was placed along the inner roadside of each horizontal curve. As illustrated in **Figure 2**, the barriers were placed at the outer edge of the road shoulder at 4 m from the road centerline and only mounted along the inner side of rightward (RW) and leftward (LW) curves.

The virtual sensor was mounted and positioned at the vehicle center of gravity. The height of the virtual sensor was 1.1 m from the road surface, consistent with the prescription from geometric policies (*26*,*27*). For validation purposes, the vehicle trajectory was fixed on the center of the driving lane to obtain the *ASD* as per the road guidelines (*26*,*27*). To reduce the noise in sensor data and to attain accurate ASD values, the maximum measured distance between the virtual sensor and the road markers was set at 300 m, which is greater than the ordinary *SD* values typically encountered in road design. The longitudinal spacing between the road markers was set at 3 m (**Figure 1a**).

For model validation, the minimum ASD for the curve is obtained when the sight line is placed along the curved section of the road and computed as follows:

$$ASD = 2R \cdot ar\cos\left[1 - \frac{d}{R}\right] \qquad (4)$$

where $R$ represents the radius of the curve and $d$ is the distance from center of the driving lane to the sight obstruction (road barrier) as illustrated in **Figure 2**.

**TABLE 2 Comparison between minimum values of actual *ASD* (estimated using Autocad®) and *ASD* values computed with the Simulink model for curves in rightward (RW) and leftward (LW) direction (*d* is the distance from the center of the driving lane to the road barrier).**

| Horizontal Curve | *R* [m] | Length [m] | Dir. | d [m] | Available Sight Distance [m] | | |
|---|---|---|---|---|---|---|---|
| | | | | | Autocad® | Sensor | Difference |
| Curve-1 | 700 | 205 | RW | 2.25 | 112.2 | 111.3 | -0.9 |
| Curve-2 | 550 | 185 | LW | 5.75 | 159.2 | 158.7 | -0.5 |
| Curve-3 | 450 | 170 | RW | 2.25 | 90 | 89.9 | -0.1 |
| Curve-4 | 350 | 150 | LW | 5.75 | 127 | 127.8 | 0.8 |
| Curve-5 | 250 | 130 | RW | 2.25 | 67.1 | 68.2 | 1.1 |
| Curve-6 | 350 | 150 | LW | 5.75 | 127 | 127.8 | 0.8 |
| Curve-7 | 265 | 135 | RW | 2.25 | 69.1 | 68.3 | -0.8 |
| Curve-8 | 190 | 120 | LW | 5.75 | 93.7 | 93.3 | -0.4 |
| Curve-9 | 130 | 105 | RW | 2.25 | 48.4 | 49.3 | 0.9 |
| Curve-10 | 85 | 90 | LW | 5.75 | 62.9 | 62.5 | -0.4 |
| Curve-11 | 50 | 75 | RW | 2.25 | 30.1 | 29.1 | -1 |

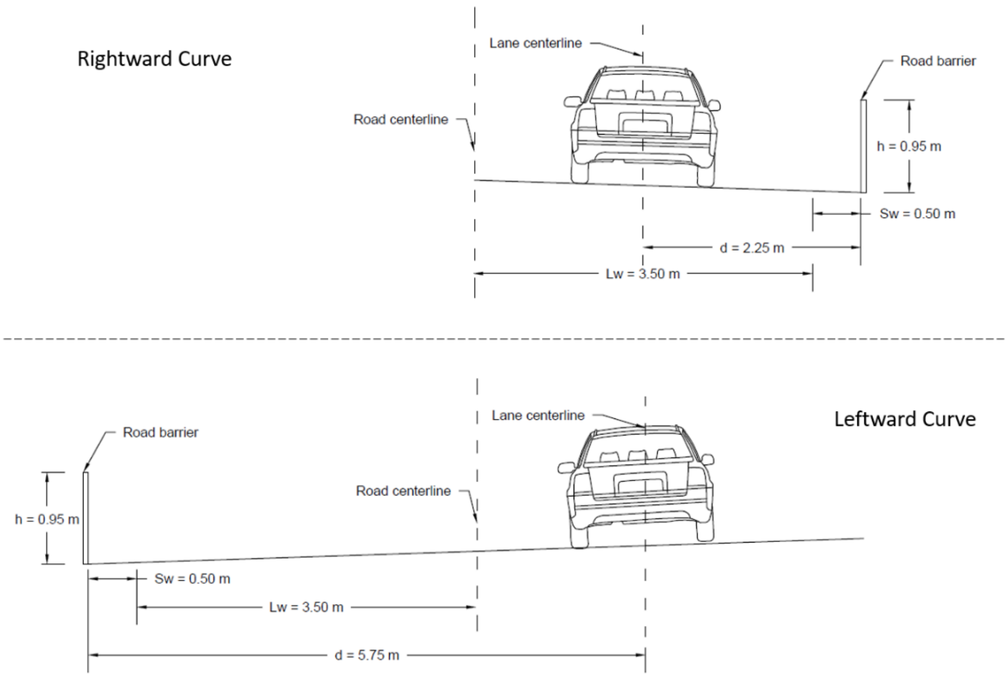


**Figure 2 Cross-section of the roadway for RW and LW direction curves (*h* = height of road barrier; *Lw* = Lane Width; *Sw* = Shoulder Width; *d* = Distance from center of driving lane to the road barrier).**

In cases where the driver point of view and/or the farthest visible road marker (**Figure 1**) fell outside the circular section of the curve, the actual *ASD* values were calculated manually for a 2D road environment using AutoCAD® software on the basis of the road's known geometrical features. The *ASD* was estimated by considering the position of the observer and target location at the lane centerline. The actual *ASD* values were estimated along the alignment having a longitudinal spacing of 5 m close to circular arcs and 15 m at straight roadway sections. The actual *ASD* was compared with the continuous values obtained from the Simulink model and it was observed that the Simulink model generated similar and precise *ASD* values as illustrated in **Figure 3**. The minimum *ASD* value for each curve was also calculated as illustrated in **Table 2**. In most cases, the absolute difference between actual *ASD* and estimated *ASD* is lower than 1 m along circular arcs.

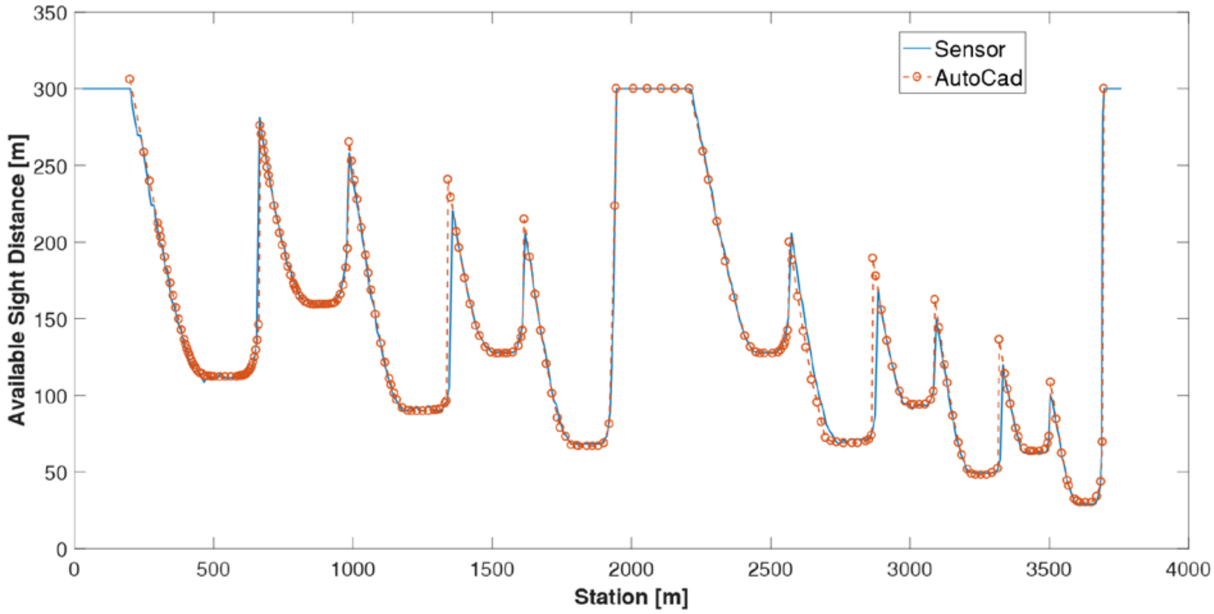


**Figure 3 Comparison between ASD values for ISA validation provided by virtual sensors in SCANeR Studio® and actual ASD values from AutoCAD®.**

## ISA TESTING

After completing the validation process, the ISA model was tested across the three different ISA variants. The driver received visual information on actual vehicle speed and the recommended safe speed based on the ASD via a display of static images showing safe and unsafe speed icons as shown in **Figure 4**. The visual information was located on the bottom left-hand corner of the main display. The visual information was positioned within 15° of the expected line of sight so that it would not distract drivers from the road ahead (*35*). In the case of ISA variant-2, a continuous auditory warning (i.e., beep) was provided as soon as the driver adopted unsafe speeds. The ISA variant-3 works with an intervening operation which either prevents the vehicle from exceeding the threshold speed limit, or intervenes automatically to decrease the vehicle speed gradually and smoothly back down from an unsafe speed to the threshold speed limit. During this operation, an icon is displayed on the main screen to inform the driver that an intervening operation has been activated by the system, as shown in **Figure 4**. To compare the results, the driver also drove under the base condition scenario without the aid of any kind of information, warning, or intervention.

In addition, the model is capable of estimating the *ASD* with respect to the longitudinal and the lateral position of the vehicle. **Figure 5** demonstrates the difference in *ASD* due to the variation in the lane gap (i.e., the lateral distance from the lane centerline) during the simulation. For instance, at station 1540 m the difference in *ASD* for ISA (Information) and ISA (Intervening) was equal to 5 m due to the respective lane gaps of -0.54 m and +0.50 m. Minor differences in ASD are to be expected, as already confirmed in Bassani et al. (*25*) who demonstrated that drivers benefit from a greater *ASD* when they increase the lateral distance from the sight obstruction.

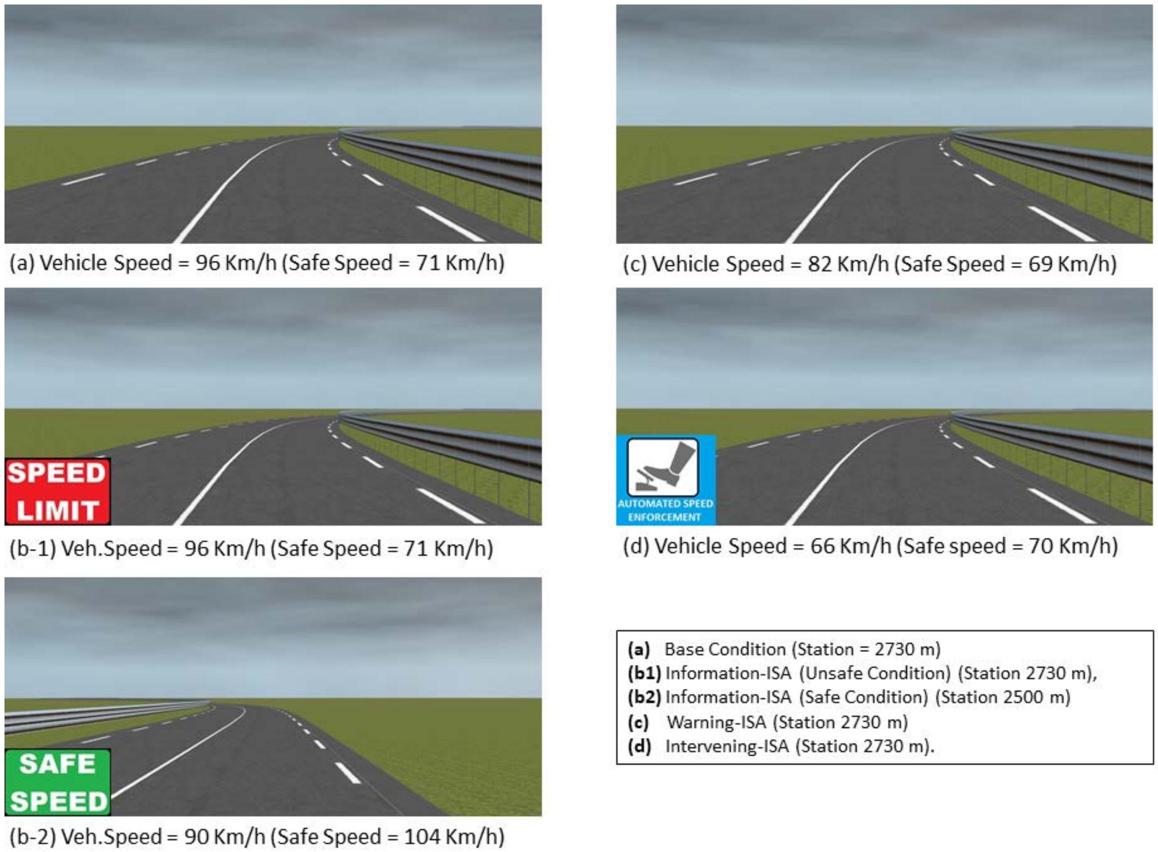


**Figure 4 Examples of visual information provided to the driver with icons for ISA variant-1 (Information), ISA variant-2 (auditory Warning), and ISA variant-3 (Intervening).**

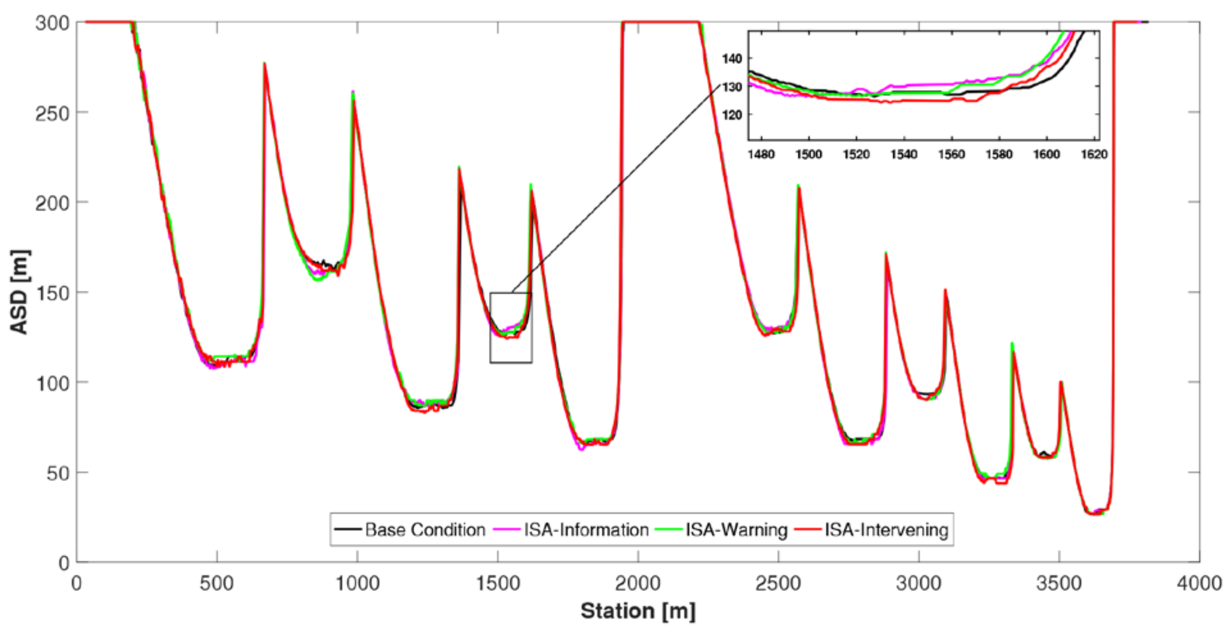


**Figure 5 ASD comparison with curves affected by the lateral position of the vehicle. A detailed representation of the different curves is provided between station 1480 and 1620 m.**

**Figure 6** provides the *ASD* and *SD* values obtained in real-time during model testing as a function of the longitudinal and lateral position of the vehicle on the road alignment. At a subsequent stage, the model converted the real-time *ASD* values (**Figure 6**) into safe/suggested speed values to implement the ISA variants as shown in **Figure 7** as per **Equation 3**. Although the *ASD* profile changes as a function of the lateral position of the vehicle, the *ASD* and safe speed values in **Figure 6** and **Figure 7** are only plotted for the ISA-intervening scenario.

In the first part of the road alignment with large curve radii (curves 1 and 2), the safe speed values are relevant due to high *ASD* values (here limited to 300 m), so there is no interaction between vehicle speed and safe speed (**Figure 7**). When the *ASD* starts decreasing along the alignment with shorter radius curves, the interaction between vehicle speed attained by the driver and suggested safe speed by the model is observed. **Figure 7** shows a decrease in speed in the case of an intervening operation under unsafe conditions ($v > v_L$). When the information and auditory warning ISA systems are in operation, drivers tend to reduce their speed to attain safer conditions. These observations support the robustness and effectiveness of the ISA system proposed here to provide information to the driver and to have feedback under unfavorable sight conditions.

In the case of Intervening operation (variant-3), the ISA system successfully and smoothly decreases the speed by disconnecting the acceleration pedal when $v > v_L$. Although it is evident that the model was not able to fully reduce the speed to the threshold speed limit, the authors will improve the algorithm by increasing the deceleration rate as per the activation of an automatic braking function in further testing.

The *ASD* and speed profiles were generated in real-time with the frequency of the Simulink model set at 100 Hz. After comparing the input and output data from the Simulink model, no potential delay or over writing of data was observed which suggests that the response time of the model was less than 1 centi-second (1/100th of a second). A lower frequency (20 Hz) was set for the output message sending frequency to avoid any network overload.

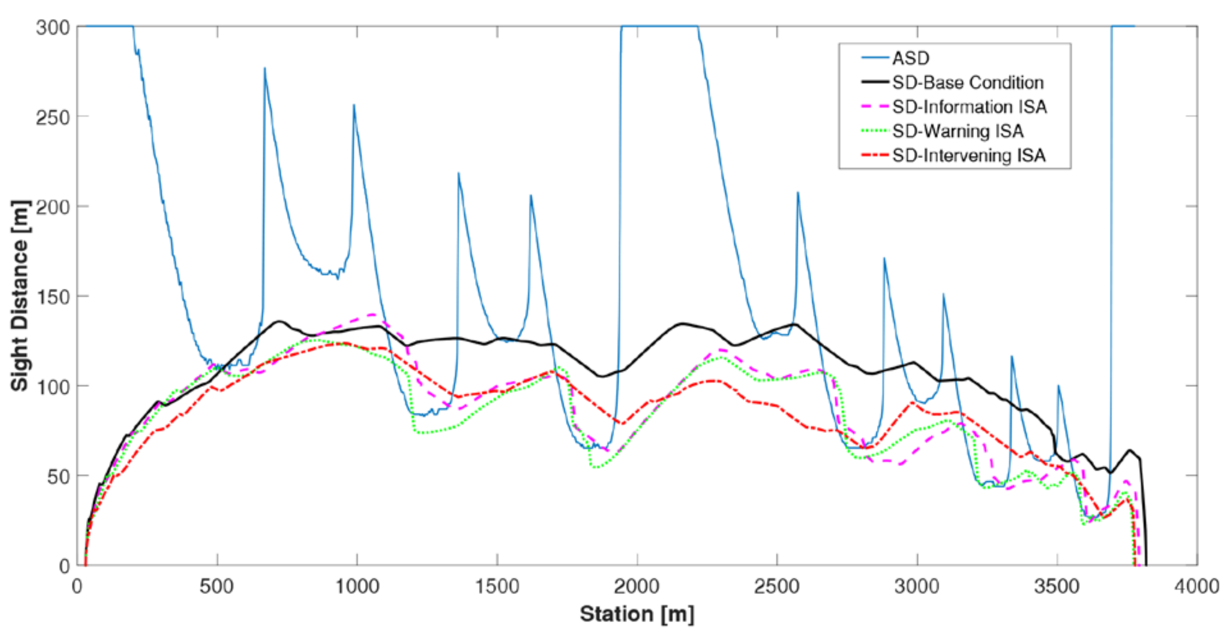


**Figure 6 Comparison between ASD and SD profiles obtained in four different drives with and without the ISA system.**

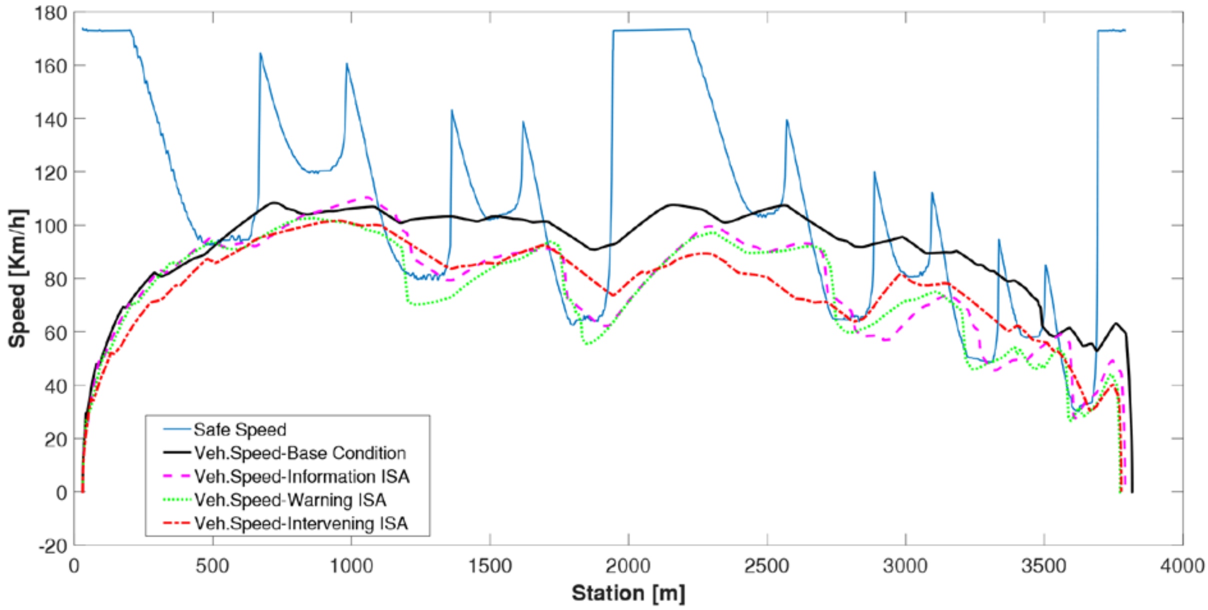


**Figure 7 Comparison between the safe speed from Equation 3 and the speed values obtained from testing under base conditions and the three ISA operations.**

## CONCLUSIONS, IMPLICATIONS AND FUTURE PERSPECTIVES

According to design standards (*26*,*27*), along roads with permanent sight obstructions (e.g., traffic barriers, vegetation, buildings, and other objects along the roadside) the available sight distance (*ASD*) must be greater than the distance required for a complete stop (i.e., the stopping distance, *SD*) in front of an unexpected obstacle, e.g. a stationary vehicle, a boulder, a fallen tree, a pedestrian crossing the lane. Unfortunately, this basic safety prescription included in current design standards is not always guaranteed in real road scenarios. Moreover, sight conditions along a road typically change due to the presence of several fixed sight obstructions that continuously alter the *ASD* from the driver's point of view. A restricted *ASD* is commonly perceived as inherently risky due to the potential presence of an unknown obstacle ahead, and in cases where the driver is traveling at high speeds, he/she might not be able to stop the car from hitting such an obstacle.

The aim of this work was to develop a virtual prototype for a novel intelligent speed adaption (ISA) system which would be effective in controlling vehicle speed along stretches of road with low ASD values. As it stands currently, the system can provide (i) onboard information to the driver, or (ii) issue warning signals when required, or (iii) trigger an automated speed control intervention (*16*). The development of this new ISA system is consistent with the simultaneous vehicle/infrastructure design (SVID) principles (*1*,*2*).

The proposed ISA system considers both the road geometrics and actual sight conditions including the presence of any sight obstructions ahead, and operates as follows:

(i) it calculates the real-time *ASD* with an onboard car sensor and compares the value obtained with the *SD* to assess the level of safety of the visibility conditions;

(ii) *ASD* values are then used by the ISA algorithm to calculate the appropriate safe speed limit relative to the actual real-time visibility along the road alignment.

In this study, *ASD* values provided by the proposed ISA were compared and validated with *ASD* values obtained from AutoCAD for flat terrain road alignment with horizontal road curves. The algorithm developed with the simulation software is capable of estimating *ASD* values from the exact location of the vehicle considering both longitudinal and lateral positions on the road.

The ensuing three information, warning, and intervening operation ISA variants developed are in line with ADAS classification (*28*,*29*). The model efficiently provided the information/warning in real-time on the main display of the simulator, and robustly acted on the accelerator pedal under the unsafe sight conditions required for an intervention operation.

Looking at it from a wider perspective, this work contributes to supporting driving operations to reach the general goals established by National and International Institutions and public Governments (e.g., Swedish and, recently, European Vision Zero) (*36*,*37*). For real applications, this particular ISA technology would require vehicles to be equipped with onboard sensors to compute ASD values. Thanks to the work of Ma et al. (*38*), the reconstructed 3D space visible with a changing line of sight for a moving observer paves the way for the introduction of the technology proposed here to the next generation of intelligent vehicles.

A natural extension to this work would be an evaluation of driving competency with the new ISA system. In future steps, the speed behavior and driver acceptance of the system will be investigated. Furthermore, indicators for situation-awareness and driver workload will be selected and analyzed by conducting experiments on a large population dataset to assess the implications of the use of this new ISA system.

While posted speed and curve warning data are not currently included in the system, future research on the interaction between the proposed novel ISA system and other ADAS modules should be of certain interest. Finally, the equipping of a real car with the novel ISA-system and its testing in a real road environment will provide an opportunity to see how the system might impact on the design of future generations of new vehicles.

**FUNDING**

This research did not receive any funds from public, commercial, or not-for-profit sectors. All activities were conducted in the Laboratory of Road Safety and Driving Simulation (RSDS Lab) at the Department of Environment, Land and Infrastructure Engineering (Politecnico di Torino, Torino, Italy).

**AUTHOR CONTRIBUTIONS**

The authors confirm contribution to the paper as follows: study conception and design: M. Bassani, A. Hazoor; model formation and data collection: A. Hazoor, A. Lioi; analysis and interpretation of results: M. Bassani, A. Hazoor; draft manuscript preparation: A. Hazoor., M. Bassani. All authors reviewed the results and approved the final version of the manuscript.

## REFERENCES


1. Harwood, d. W. (1998). Simultaneous vehicle/infrastructure design: highway infrastructure perspective (no. E-c001 appendix). Available at: https://trid.trb.org/view/477847 (Accessed April 5th, 2020).

2. Larson, T. D. (1998). Simultaneous vehicle/infrastructure design: an overview. SVID applications and benefits to the total transportation system (no. E-c001 appendix).

3. Aarts, L., and Van Schagen, I. (2006). Driving speed and the risk of road crashes: A review. *Accident Analysis and Prevention*, 38(2):215-224.

4. Nilsson, G. (2004). Traffic safety dimensions and the power model to describe the effect of speed on safety (Doctoral dissertation, Univ.).

5. Hauer, E. (2009). Speed and safety. *Transportation Research Record: Journal of the Transportation Research Board*, 2103(1):10-17.

6. Li, H., Zhu, M., Graham, D. J., and Zhang, Y. (2020). Are multiple speed cameras more effective than a single one? Causal analysis of the safety impacts of multiple speed cameras. *Accident Analysis and Prevention*, 139:105488.

7. Comte, S. L., and Jamson, A.H. (2000). Traditional and innovative speed-reducing measures for curves: an investigation of driver behaviour using a driving simulator. *Safety Science*, 36(3):137-150.

8. Mountain, L. J., Hirst, W. M., and Maher, M. J. (2005). Are speed enforcement cameras more effective than other speed management measures? The impact of speed management schemes on 30 mph roads. *Accident Analysis and Prevention*, 37(4):742-754.

9. Young, K. L., Regan, M. A., Triggs, T. J., Jontof-Hutter, K., and Newstead, S. (2010). Intelligent speed adaptation—Effects and acceptance by young inexperienced drivers. *Accident Analysis and Prevention*, 42(3):935-943.

10. Høye, A. (2014). Speed cameras, section control, and kangaroo jumps–a meta-analysis. *Accident Analysis and Prevention*, 73:200-208.

11. Freeman, J., Kaye, S. A., Truelove, V., and Davey, J. (2017). Is there an observational effect? An exploratory study into speed cameras and self-reported offending behaviour. *Accident Analysis and Prevention*, 108:201-208.

12. Hirst, W. M., Mountain, L. J., and Maher, M. J. (2005). Are speed enforcement cameras more effective than other speed management measures? An evaluation of the relationship between speed and accident reductions. *Accident Analysis and Prevention*, 37(4):731-741.

13. Li, H., and Graham, D. J. (2016). Heterogeneous treatment effects of speed cameras on road safety. *Accident Analysis and Prevention*, 97:153-161.

14. Carsten, O. M., and Tate, F. N. (2005). Intelligent speed adaptation: accident savings and cost–benefit analysis. *Accident Analysis and Prevention*, 37(3):407-416.

15. Spyropoulou, I. K., Karlaftis, M. G., and Reed, N. (2014). Intelligent Speed Adaptation and driving speed: Effects of different system HMI functionalities. *Transportation Research Part F: Traffic Psychology and Behaviour*, 24:39-49.

16. Lai, F., and Carsten, O. (2012). What benefit does Intelligent Speed Adaptation deliver: A close examination of its effect on vehicle speeds. *Accident Analysis and Prevention*, 48:4-9.

17. Elvik, R., Høye, A., Vaa, T., and Sørensen, M. (2009). *The Handbook of Road Safety Measures*. Second Edition. Emerald Group Publishing Limited.

18. OECD (2006). Speed Management. Paris: OECD. Joint Transport Research Committee, Paris.

19. Gayah, V. V., Donnell, E. T., Yu, Z., and Li, L. (2018). Safety and operational impacts of setting speed limits below engineering recommendations. *Accident Analysis and Prevention*, 121:43-52.

20. Gargoum, S. A., El-Basyouny, K., and Kim, A. (2016). Towards setting credible speed limits: Identifying factors that affect driver compliance on urban roads. *Accident Analysis and Prevention*, 95:138-148.

21. Goldenbeld, C., and Van Schagen, I. (2007). The credibility of speed limits on 80 km/h rural roads: the effects of road and person(ality) characteristics. *Accident Analysis and Prevention*, 39(6):1121–1130.

22. Gargoum, S. A., El-Basyouny, K., and Sabbagh, J. (2018). Assessing stopping and passing sight distance on highways using mobile LiDAR data. *Journal of Computing in Civil Engineering*, 32(4):04018025.

23. Bassani, M., Grasso, N., and Piras, M. (2015). 3D GIS Based Evaluation of the Available Sight Distance to Assess Safety of Urban Roads. *International Archives of the Photogrammetry, Remote Sensing and Spatial Information Sciences*, 40 -3/W3:137-143.

24. Jung, J., Olsen, M. J., Hurwitz, D. S., Kashani, A. G., and Buker, K. (2018). 3D virtual intersection sight distance analysis using lidar data. *Transportation Research Part C: Emerging Technologies*, 86:563-579.

25. Bassani, M., Hazoor, A., and Catani, L. (2019). What's around the curve? A driving simulation experiment on compensatory strategies for safe driving along horizontal curves with sight limitations. *Transportation Research Part F: Traffic Psychology and Behaviour*, 66:273-291.

26. AASHTO (2018). *A Policy on Geometric Design of Highways and Streets* (7th Edition). American Association of State Highway, and Transportation Officials, Washington, D.C.

27. MIT (2001). *Norme funzionali e geometriche per la costruzione delle strade* (in Italian). Ministero delle Infrastrutture e dei Trasporti, D.M. no. 6792 of November 5th.

28. Carsten, O. (2002). European research on ISA: Where are we now and what remains to be done. ICTCT, Nagoya.

29. Winner, H., Hakuli, S., Lotz, F., & Singer, C. (Eds.). (2014). *Handbook of driver assistance systems*. Springer International Publishing.

30. Catani, L. (2019). A Simulation Based Study on Driver Behavior when Negotiating Curves with Sight Limitations. Doctoral dissertation, Politecnico di Torino, Turin, Italy.

31. Bassani, M., Catani, L., Ignazzi, A.A., and Piras, M. Validation of a Fixed-Base Driving Simulator to Assess Behavioural Effects of Road Geometrics. Presented at the DSC 2018 EUROPE VR Driving Simulation Conference & Exhibition (pp. 101–108). Antibes, France.

32. Catani, L. and Bassani, M. Anticipatory Distance, Curvature, and Curvature Change Rate in Compound Curve Negotiation: A Comparison between Real and Simulated Driving. Presented at 98th Annual Meeting of the Transportation Research Board, Washington, D.C., 2019.

33. Karimi, A., Bassani, M., Boroujerdian, A. M., and Catani, L. (2020). Investigation into passing behavior at passing zones to validate and extend the use of driving simulators in two-lane roads safety analysis. *Accident Analysis and Prevention*, 139:105487.

34. Khastgir, S., Birrell, S., Dhadyalla, G., and Jennings, P. Development of a drive-in driver-in-the-loop fully immersive driving simulator for virtual validation of automotive systems. Presented at 2015 IEEE 81st Vehicular Technology Conference (VTC Spring) (pp. 1-4). IEEE.

35. NHTSA (2007). Crash Warning System Interfaces: Human Factors Insights and Lessons Learned. U.S Department of Transportation; National Highway Traffic Safety Administration.

36. Johansson, R. (2009). Vision Zero–Implementing a policy for traffic safety. *Safety Science*, 47(6):826-831.

37. European Commission (2019): COMMISSION STAFF WORKING DOCUMENT, EU Road Safety Policy Framework 2021-2030 -Next steps towards "Vision Zero", (accessed 2 Nov 2019): https://ec.europa.eu/transport/themes/strategies/news/2019-06-19-vision-zero_en

38. Ma, Y., Zheng, Y., Cheng, J., and Easa, S. (2019). Real-time visualization method for estimating 3D highway sight distance using LiDAR data. *Journal of Transportation Engineering, Part A: Systems*, 145(4):04019006.